Probing a Potassium Channel Pore with an Engineered Protonatable Site†

Zhe Lu and Roderick MacKinnon*

Department of Neurobiology, Harvard Medical School, 220 Longwood Avenue, Boston, Massachusetts 02115

Received May 30, 1995; Revised Manuscript Received August 10, 1995⊗

ABSTRACT: Blockade by intracellular cations reduces outward conduction of K^+ in inward rectifier K^+ channels. Mutations of residue 171 in the second transmembrane (M2) segment of the ROMK1 channel have been found to affect the affinity for blockade by intracellular Mg^{2+} and polyamines. In the present study, we examined the mechanism by which this residue mediates blockade by placing a proton acceptor (histidine) at this position. The results allow us to draw two conclusions. First, the side chain of residue 171 is located in the ion conduction pore about halfway across the transmembrane voltage drop. Second, its side chain comes into close contact and interacts electrostatically with a blocking ion.

Certain K^+ channels support a large conductance when K^+ flows into the cell and a small conductance when K^+ flows out of the cell. This property, called inward rectification, is important for the biological role of these K^+ channels (Hille, 1991). One basis for inward rectification is voltage-dependent blockade by intracellular cations: Impermeant cations such as Mg^{2+} and polyamines bind along the ion conduction pathway under conditions where K^+ would otherwise flow out of the cell (Horie et al., 1987; Matsuda et al., 1987; Vandenberg, 1987; Ficker et al., 1994; Lopatin et al., 1994; Fakler et al., 1995). Cloned inward rectifier K^+ channels displaying different degrees of rectification have provided a basis for identifying the binding sites for the blocking cations (Ho et al., 1993; Kubo et al., 1993a,b; Dascal et al., 1993; Ashford et al., 1994; Stanfield et al., 1994; Lu & MacKinnon, 1994; Wible et al., 1994; Ficker et al., 1994; Lopatin et al., 1994; Fakler et al., 1995).

A single subunit of inward rectifier K^+ channels is thought to contain two main membrane-spanning stretches (M1 and M2) flanking a P (pore) region (Ho et al., 1993; Kubo et al., 1993a). Based on voltage-activated K^+ channels (MacKinnon, 1991; Liman et al., 1992; Li et al., 1994), we expect four subunits to surround a central pore. The P regions reach into the pore and form a selectivity filter (Heginbotham et al., 1992, 1994; De Biasi et al., 1993; Kirsh et al., 1995). Mutations at a residue in the M2 stretch have been shown to affect the binding of intracellular cationic blockers. In the ROMK1 inward rectifier channel, mutation of asparagine to aspartate at position 171 in M2 increased the blocking affinity of Mg^{2+} and polyamines (Lu & MacKinnon, 1994; Wible et al., 1994; Ficker et al., 1994; Lopatin et al., 1994). Mutation of the corresponding residue in another inward rectifier channel, IRK1, from aspartate (Asp)[1] to amino acids with a neutral side chain reduced the affinity of the cationic blockers (Stanfield et al., 1994; Ficker et al., 1994; Lopatin et al., 1994; Fakler et al., 1995). These findings indicate that the amino acid at position 171 (in ROMK1) interacts with ions in the conduction pore. What is the mechanism by which substitutions at this position affect the affinity of a blocking ion? To address this question, we engineered a specific protonatable site by substituting histidine (His) at position 171. Analysis of the interaction of protons with this site leads us to conclude that amino acid 171 is located in the ion conduction pathway and that its side chain comes into intimate contact with ions in the pore.

MATERIALS AND METHODS

Molecular Biology and Oocyte Preparation. DNA encoding the ROMK1 channel was cloned into the p-SPORT1 plasmid (Gibco-BRL, Gathersbury, MD; Ho et al., 1993). Mutations were generated by replacing a segment of DNA (*Nde*1−*Bgl*II; 310−691) with a sequenced PCR-cassette containing the mutation. RNA was synthesized from *Not*1 (NEB, Cambridge, MA)-linearized DNA using T7 polymerase (Promega Corp., Madison, WI). Oocytes from *Xenopus laevis* were incubated in solution containing (mM) 82.5 NaCl, 2.5 KCl, 1 $MgCl_2$, 5 HEPES, pH 7.6, and collagenase (2−4 mg/mL; Gibcol-BRL) for 90−120 min. The oocytes were then rinsed thoroughly and stored in an incubating solution containing (mM) 96 NaCl, 2 KCl, 1.8 $CaCl_2$, 1 $MgCl_2$, 5 HEPES, pH 7.6, and gentamicin (50 μg/mL). Defolliculated oocytes were selected at least 2 h after collagenase treatment. RNA was injected at least 16 h later. After injection of RNA, oocytes were placed in an incubator at 18 °C.

Electrophysiological Recording. Tight-seal patch recording (Axopatch, 2B; Axon Instruments, Inc., Foster City, CA) was performed 2−6 days after the injection of RNA. Macroscopic $I-V$ curves were recorded from patches with many (100−300) channels while ramping membrane voltage from −100 mV to 100 mV over a duration of 1−4 s. Data were filtered at 0.2−1 kHz and sampled every 2−7.8 ms using an analog to digital converter (Indec Systems, Inc., Sunnyvale, CA) interfaced with a 386 personal computer. At the end of each experiment, patches were exposed to a solution containing 2−3 mM Mg^{2+} without ATP to induce the disappearance of functional channels. The records obtained after the channels disappeared were taken as a template for leak subtraction (Lu & MacKinnon, 1994).

Single channel currents were recorded by excising inside-out (or outside-out) patches from devitellinized oocytes. The

† This work was supported by NIH Grant GM 47400 to R.M.

* Address correspondence to this author at the Department of Neurobiology, Harvard Medical School, 220 Longwood Ave., Boston, MA 02115. Telephone: 617-432-1758. FAX: 617-734-7557.

⊗ Abstract published in *Advance ACS Abstracts,* September 15, 1995.

[1] Abbreviations: Asn, asparagine; Asp, aspartate; Glu, glutamate; His, histidine; D_2O, deuterium oxide.

0006-2960/95/0434-13133$09.00/0

single channel data were filtered at 1 kHz and sampled every 140 μs. The open and closed dwell time durations were measured using a 50% threshold with a cutoff time of 0.56 ms. Open dwell time distributions were fit with a single exponential function. The time constant agreed well with the mean open time.

Recording Solutions. Pipe (external) solutions contained (mM) 100 K^+ (Cl^- as the main counter-ion), 0.3 $CaCl_2$, 1 $MgCl_2$, and 10 HEPES (pH 7.1). In the low-K^+ solutions, Na^+ was used to substitute K^+ such that the concentration of K^+ and Na^+ together was 100 mM. Internal solutions contained (mM) 100 K^+ (Cl^- as the main counterion), 5 EDTA, and 10 HEPES. The pH was adjusted to the desired value using KOH. Mg^{2+}-containing internal solution for inducing channel disappearance contains 0.5 mM EGTA (no EDTA) and 2−3 mM Mg^{2+}. To study the deuterium isotope effect, solutions were made using D_2O. All pH values reported for both H_2O and D_2O solutions were those directly measured using an Orion pH meter (Model 720) with a Corning glass electrode (no. 476540).

RESULTS

Histidine Substitution Renders the Channel Sensitive to Intracellular Protons. The conductance of the wild-type ROMK1 K^+ channel is only weakly affected by changes in the intracellular pH (Figure 1A). When a His replaces the wild-type Asn at position 171, the current−voltage curve becomes strongly dependent on intracellular pH (Figure 1B). At pH 9, the curve is nearly linear while at pH 7 conductance is greater in the inward than in the outward direction (i.e., it inwardly rectifies). This could be explained if protons block the channel from the intracellular solution in a voltage-dependent manner. The fraction of unblocked current measured at different proton concentrations, relative to that measured at pH 9, is shown for several voltages (Figure 2A). The proton affinity increases (pK_a increases) as the membrane voltage is made more positive, as if protons are being driven to a site in the pore. In Figure 2B, the pK_a values ($-\log K_i$), determined as in Figure 2A, are plotted as a function of membrane voltage. The voltage dependence suggests that a proton crosses 40% of the transmembrane voltage when it travels from the intracellular solution to its binding site in the pore. The estimated pK_a of the site at 0 mV is 7.7. Changes in extracellular pH (7.0−9.0) have only a minimal effect on conductance (Figure 1C).

Microscopic Analysis of Proton Blockade. Figure 3A shows single channel current traces recorded at three different pH values. In these traces, K^+ flows inward (downward deflection from the zero current dashed line). Nonconducting intervals (deflections to the dashed line) are rare at pH 8 but increase in frequency as the pH is lowered to 7. This observation implies that a proton binds and induces a nonconducting state. That is, a nonconducting interval corresponds to a time when a proton is blocking the channel. Dwell time histograms of the conducting intervals are shown beside each trace (Figure 3B), and the reciprocal of the time constant for a single exponential fit to the histogram is graphed as a function of proton concentration (Figure 4). The time constant reciprocal corresponds to the aggregate first-order rate constant for leaving the conducting state. In the limit of zero proton concentration, the rate constant for exit from the conducting state is about 70 s^{-1}. This value

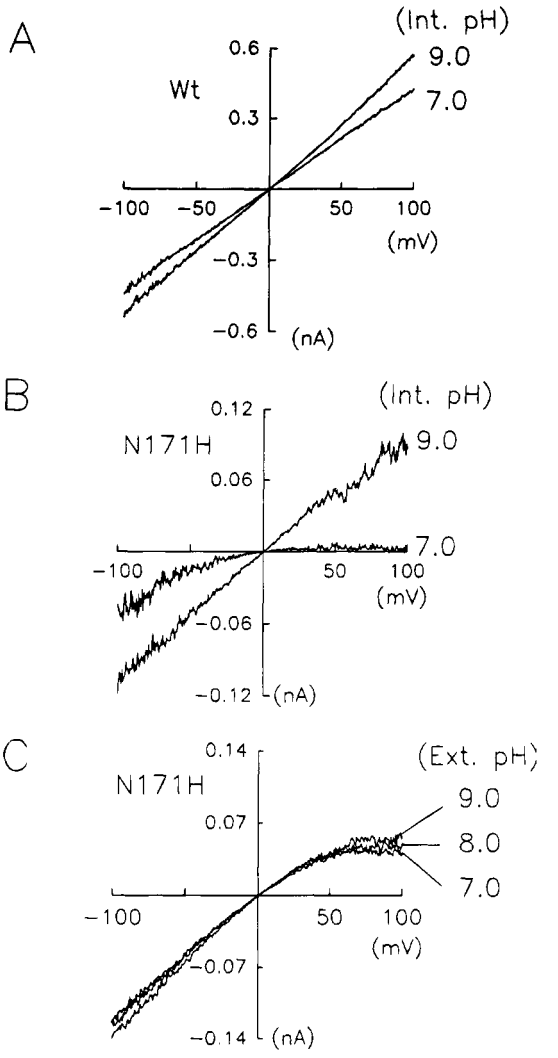

FIGURE 1: Intracellular protons block outward current in the histidine mutant channel. (A) Lowering the pH from 9 to 7 in the wild-type channel causes only a slight reduction in current at all voltages. (B) A mutant channel with His 171 is sensitive to internal but not to external pH (C). Currents were recorded from patches containing many channels while ramping membrane voltage from −100 mV to 100 mV. (Voltages are reported relative to ground on the extracellular side of the membrane.) The data in (A) and (B) are from a single ramp while those in (C) are an average of four ramps. Solutions contained 100 mM KCl on both sides of the patch as described under Materials and Methods. Records from (A) and (B) were made in inside-out patches and (C) in an outside-out patch. Intracellular pH in (C) was 8.0.

corresponds to a proton-independent event (for example, channel closing). The linear increase in the rate constant as a function of proton concentration provides us with a second-order proton association rate constant (slope) of 1.9×10^9 M^{-1} s^{-1}.

Because two processes (proton-independent channel closing and proton-dependent blockade) lead to indistinguishable nonconducting states, we expect the distribution of nonconducting intervals to be more complicated than a single exponential. Nevertheless, Figure 4 shows that the first-order rate constant for entry into a nonconducting state at pH 8 is only 20% greater than in the zero proton limit. Therefore, 80% of nonconducting events at pH 8 are due to closing and not protonation: From such records, we estimate the rate constant for channel opening to be about 400 s^{-1}. At pH 7, where 70% of the nonconducting events are due to

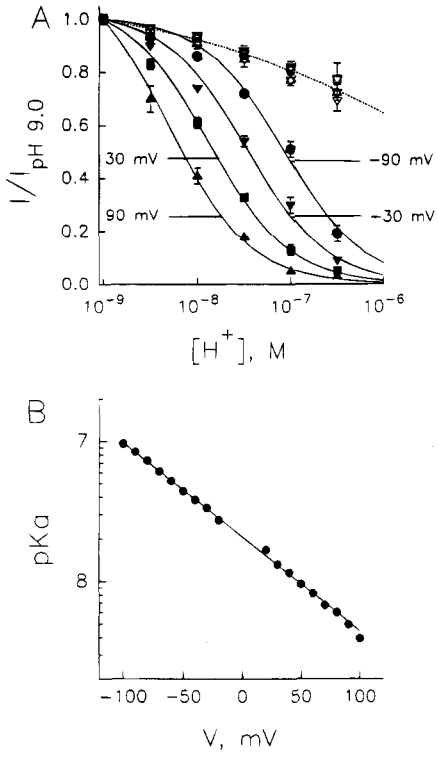

FIGURE 2: Proton block of the His mutant channel is voltage-dependent. (A) The fraction of unblocked current (compared to that measured at pH 9.0), $I/I_{pH\ 9.0}$, is plotted against the corresponding proton concentration (filled symbols: His mutant channel). Measurements made at four different membrane voltages (indicated on graph) are shown. Each symbol is the mean ± SEM ($n = 3-7$) of measurements made in separate patches. The curves superimposed on the data correspond to least-squares fits to the equation: $I/I_{pH\ 9.0} = [K_i(V) + 10^{-9}]/(K_i(V) + [H^+])$. $K_i(V)$ is the K_i at membrane voltage V. The open symbols show data for the wild-type channel measured from four different patches under the same conditions. (B) pK_a (−log K_i) for the His mutant channel determined in (A) is plotted against the corresponding membrane voltage. The line superimposed on the data is a least-squares fit to $K_i(V) = K_i(0)\exp(-\delta FV/RT)$. The fit gives a $K_i(0)$ of 2.1×10^{-8} M and a δ of 0.4.

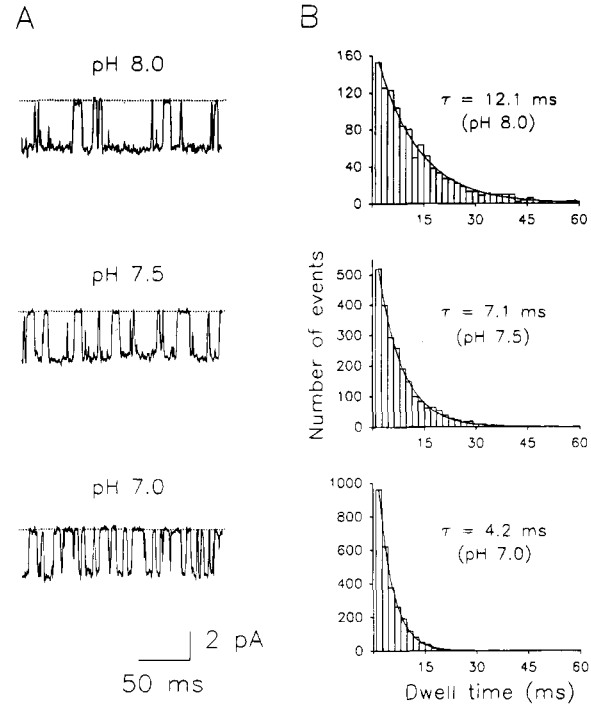

FIGURE 3: Single channel analysis of proton blockade. (A) Single channels were recorded from inside-out patches in 100 mM KCl solutions with different internal (bath) pH values (indicated above traces). Dashed lines show the closed channel current level. (B) Dwell time histograms (bin width 1.8 ms) for the open (conducting) levels are shown for the same three pH values. A single exponential function was fit (least squares) to each histogram, and the time constant is shown. Channel records were recorded at −80 mV. External (pipet) solution was pH 7.1.

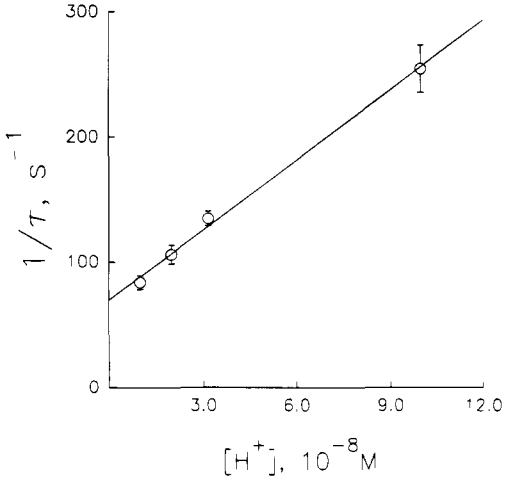

FIGURE 4: Estimating the rate constant for proton transfer to His 171. The time constants for the conducting intervals (Figure 3) were determined at several pH values, and their reciprocal is plotted as a function of proton concentration. Each point shows the mean ± SEM of 4−6 separate determinations. The solid line (least squares) corresponds to the equation $k = k_{closing} + \alpha[H^+]$, where $k_{closing}$ is the proton-independent first-order rate constant for channel closing and α is the second-order rate constant for proton transfer to the channel. $k_{closing}$ is about 70 s^{-1}, and α is 1.9×10^9 M^{-1} s^{-1}. Recording conditions were identical to those in Figure 3.

protonation, the nonconducting durations are roughly 2 times longer than at pH 8. The deprotonation rate constant is therefore about 200 s^{-1}.

Deuterium Isotope Effect on Protonation. To investigate the rate-limiting step in proton-induced blockade, we carried out experiments in solutions prepared using D_2O. Deuterium ions and protons inhibit the channel with a similar pK_a and voltage dependence (Figure 5A−C). We must, however, take into account the overestimation of deuterium ion concentration by a glass pH electrode. A more accurate estimation of the deuterium ion concentration is obtained by adding 0.4 pH unit to the measured value (Jencks, 1987). Therefore, deuterium ions bind to the site in the channel with about 3-fold higher affinity. Inspection of single channel records reveals a fairly prominent kinetic isotope effect: Transition rates between the conducting and nonconducting states are slower in the D_2O solutions (Figure 5D,E). Most of the effect on the rate of proton association is due to the overestimation of the deuterium ion concentration by the glass pH electrode. But the slowed rate of deprotonation is due to a true kinetic isotope effect.

Extracellular K^+ Affects the Affinity of Intracellular Protons. Figure 6A shows proton blocking curves in the presence of 40 mM or 100 mM extracellular K^+. The proton affinity decreases 2-fold as K^+ is increased over this range with little effect on the voltage dependence (Figure 4B). Single channel recordings show that extracellular K^+ concentration influences the length of the nonconducting intervals but not the conducting intervals (Figure 6C,D). These results imply that K^+ from the extracellular solution enters

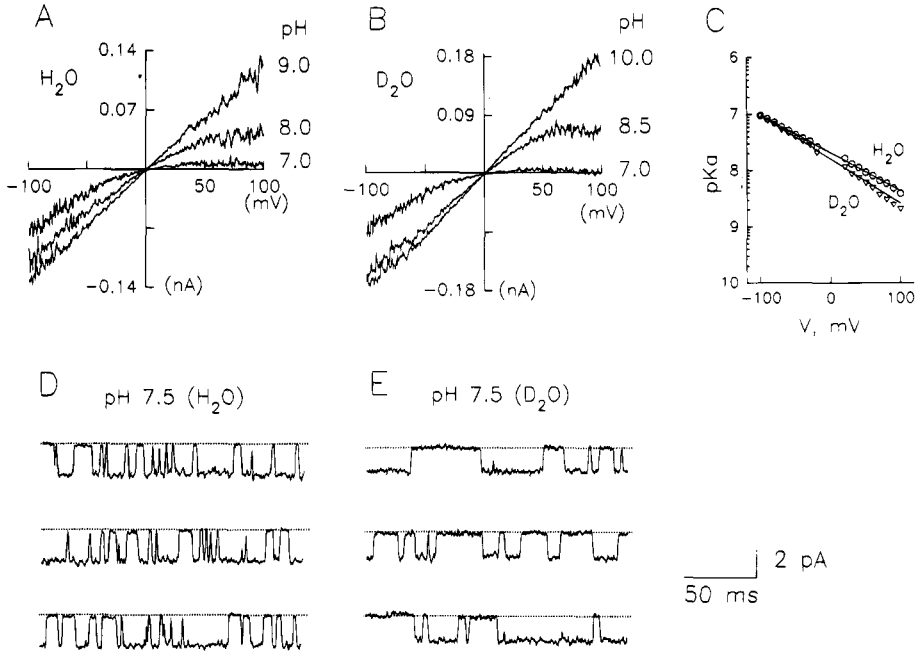

FIGURE 5: Deuterium isotope effect on protonation of His 171. (A) Current−voltage curves were recorded at three different internal (bath) pH values from inside-out membrane patches containing many His 171 mutant channels while ramping the voltage from −100 mV to 100 mV. (B) In a separate patch, a similar experiment was carried out in solutions prepared using D_2O. The reported pH values for both H_2O and D_2O solutions were directly measured using a glass pH electrode (see Materials and Methods and Results). (C) pK_a (−log K_i) for proton block was determined as shown in Figure 2A and is plotted as a function of membrane voltage for H_2O (circles) and D_2O (triangles) solutions. For the data from H_2O solutions, K_i was determined from a plot of $I/I_{pH\ 9.0}$ as described in Figure 2A. In D_2O, the data were fit to $I/I_{pH\ 10.0}$. The solid lines correspond to fits (least squares) to the equation $K_i(V) = K_i(0)\ exp(-\delta FV/RT)$. The fits give $K_i(0) = 2.1 \times 10^{-8}$ M and $\delta = 0.4$ for H^+, and $K_i(0) = 1.6 \times 10^{-8}$ M and $\delta = 0.46$ for D^+. (D, E) Single channels were recorded in 100 mM KCl solutions prepared in H_2O (D) and D_2O (E) at the indicated internal pH values. External pH was 7.1, and voltage was −80 mV.

the pore and destabilizes a proton on its binding site, causing it to dissociate at a higher rate.

DISCUSSION

The importance of amino acid 171 in the ROMK1 channel (and the corresponding residue in homologous K^+ channels) in determining the affinity of blocking ions that underlie inward rectification is well established (Stanfield et al., 1994; Lu & MacKinnon, 1994; Wible et al., 1994; Ficker et al., 1994; Lopatin et al., 1994; Fakler et al., 1995). By studying a channel with His 171, we have been able to look in greater mechanistic detail at how an amino acid at this position affects blocking ions in the pore. The His residue renders the channel sensitive to pH. Intracellular protons induce discrete interruptions of the single channel current. The effects of transmembrane voltage and extracellular K^+ on proton inhibition are signatures of an open channel blocker: Protons presumably block ion conduction by binding to His 171 in the pore.

How many protons are needed to block the channel? The question arises because the K^+ channel in these experiments is a homomultimer and the mutation is present in all (probably four) subunits. The pseudo-first-order association rate constant (Figure 4) is a linear function of the proton concentration, implying that one proton is sufficient to block ion conduction. Although one might imagine that a second proton could enter the already blocked channel, the data are most compatible with a one proton per channel stoichiometry. For example, Figure 7 shows data from a proton blocking experiment with curves corresponding to models where one or two protons can bind in the pore. As the affinity of the second proton is decreased, the curves better fit the data. The fit is best when a second proton never enters. Although we assume there are four His side chains in the pore, protonation of the first may perturb the pK_a of the remaining three so that they remain unprotonated over the pH range studied. The assumption of pK_a perturbation contrasts with results from a cyclic nucleotide-gated channel where two equivalent and independent (no perturbation) protonatable sites have been described (Root & MacKinnon, 1994).

The second-order rate constant for proton block ($1.9 \times 10^9\ M^{-1}\ s^{-1}$) is 10−100 times smaller than that for a typical diffusion-limited proton transfer reaction. Does this mean that proton transfer is not rate-limiting? The linear dependence on proton concentration of the pseudo-first-order inhibition rate constant (Figure 4) as well as the kinetic isotope effect (Figure 5) indicates that proton transfer is at least partially rate-limiting. The relatively small rate constant may be due to a limited access pathway since the proton must enter the pore to reach its site.

Metal ions like Ba^{2+} or Mg^{2+} block a K^+ channel because they lodge in the conduction pathway and disrupt the flow of ions. The observation that *extracellular* K^+ influences the affinity of *intracellular* protons argues that protons also inhibit by entering the pore. But protons must be viewed differently because they are transferred from hydronium ions to the His imidazole. An economical explanation for proton block is given by proposing that residue 171 is located in a relatively narrow part of the ion conduction pore. When His 171 is protonated and becomes positively charged, it repels other cations. As a consequence, the flow of K^+ is disrupted. This view is compatible with the above suggestion that protonation of the first of four His residues (one from each subunit) may perturb the pK_a of the other three so they

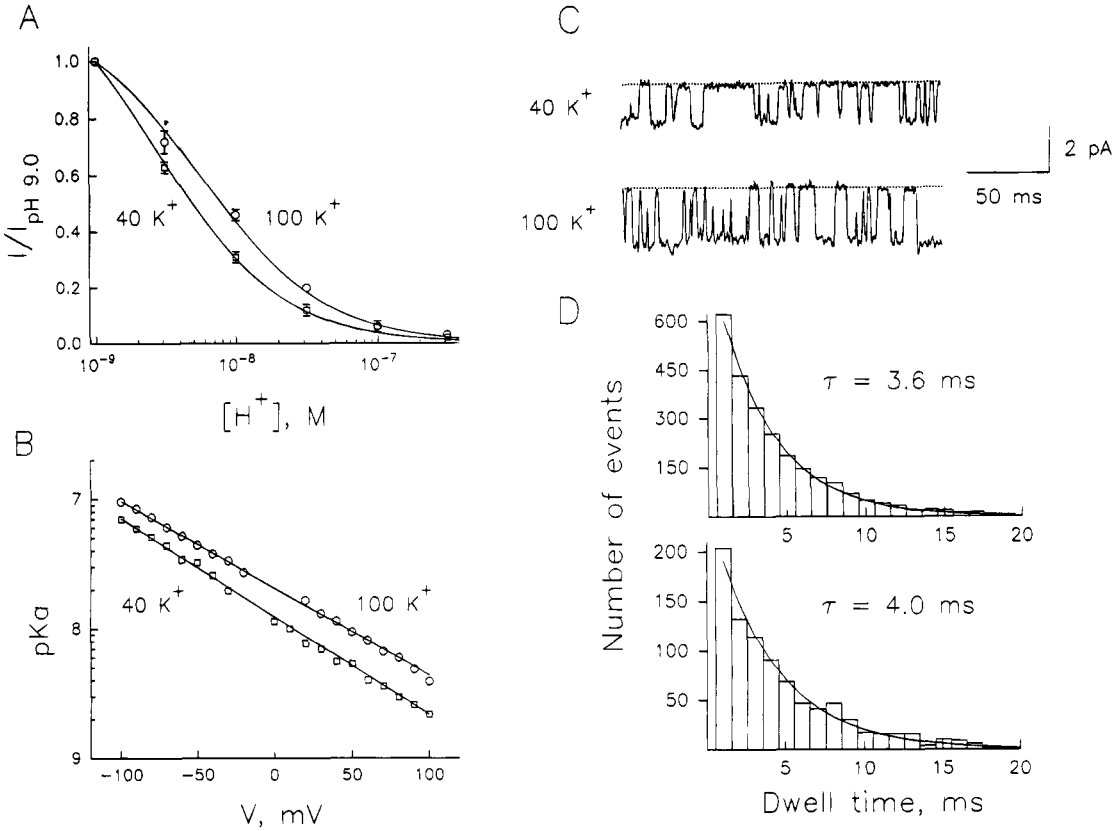

FIGURE 6: Effect of extracellular K^+ concentration on proton blockade. (A) $I/I_{pH\ 9.0}$ (mean ± SEM; $n = 4-5$) is plotted against the corresponding proton concentration for two extracellular K^+ concentrations (40 and 100 mM). The data were collected at 80 mV. The curves correspond to fits (least squares) to the equation $I/I_{pH\ 9.0} = [K_i(V) + 10^{-9}]/[K_i(V) + [H^+]]$. The estimated K_i(40 K^+) and K_i(100 K^+) for proton block are 3.0×10^{-9} M and 6.0×10^{-9} M, respectively. The K_i versus membrane voltage values for the two conditions are plotted in (B). The lines correspond to equation $K_i(V) = K_i(0\ mV) \exp(-\delta FV/RT)$ with K_i(0 mV, 40 K^+) $= 1.2 \times 10^{-8}$ M, δ(40 K^+) = 0.44, K_i(0 mV, 100 K^+) $= 2.1 \times 10^{-8}$ M, and δ(100 K^+) = 0.4. (C) Single channel current traces were recorded in the presence of either 40 mM or 100 mM extracellular K^+ at −80 mV (pH 7.0). The dashed lines show the zero-current level. The corresponding open time histograms (bin width 1.0 ms) are illustrated (D). The curves are single exponential fits (least squares) with time constants indicated on the graphs.

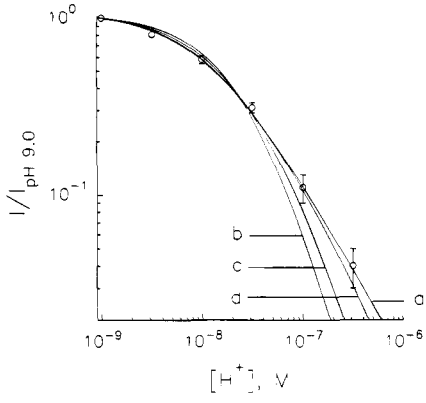

FIGURE 7: Protons appear to block the channel with 1:1 stoichiometry. $I/I_{pH\ 9.0}$ is plotted against the corresponding proton concentration. Each point is the mean ± SEM of four independent measurements made at 60 mV. The four different curves are based on models where a single proton is able to block the channel but a second proton enters with a different affinity. Model a assumes that a second proton never enters, b assumes that a second enters with the same K_i as the first, and c and d assume that a second enters with a 10-fold and 100-fold lower affinity than the first.

remain unprotonated over the pH range studied.

The results of this study firmly place amino acid 171 in the ion conduction pore. The affinity of a specific blocker depends on the residue at this position. His 171 renders the channel sensitive to protons, and Asp and Glu render it more sensitive to Mg^{2+} (Lu & MacKinnon, 1994; Wible et al., 1994). It is reasonable to conclude that this amino acid is in a position to form an ion binding site along the ion conduction pathway. It is interesting to note that the voltage dependence of Mg^{2+} block (in a channel with Asp 171) is about twice that of proton block (in a channel with His 171) (Figure 2; Lu & MacKinnon, 1994). The difference in valence of these two blocking ions can account for the different voltage dependences, as if the Mg^{2+} and proton sites in the respective channels are at the same position along the pore.

This study asked how the amino acid at position 171 affects the affinity of a blocking cation. Our ability to produce a proton blocking site by introducing a histidine argues that its side chain comes into close contact and interacts electrostatically with a blocking ion. The developing picture of a K^+ channel is that of a transmembrane pore with a selectivity filter formed by pore loops reaching into the pore from the extracellular side (MacKinnon, 1995). Residue 171 must be located internal to the selectivity filter since it interacts much more effectively with blocking cations from the inside.

ACKNOWLEDGMENT

We thank C.-S. Park, M. Root, and K. Swartz for helpful discussions.

REFERENCES

Ashford, M. L. J., Bond, C. T., Blair, T. A., & Adelman, J. P. (1994) *Nature 370*, 456−459.

Dascal, N., Schreibmayer, W., Lim, N. F., Wang, W., Chavkin, C., DiMagno, L., Labarca, C., Kieffer, B. L., Gaveriaux-Ruff, C., Trollinger, D., Lester, H., & Davison, N. (1993) *Proc. Natl. Acad. Sci. U.S.A. 90*, 10235−10239.

De Biasi, M., Drewe, J. A., Kirsch, G. E., & Brown, A. M. (1993) *Biophys. J. 65*, 1235−1242.

Fakler, B., Brandle, U., Glowatzki, E., Weidemann, S., Zenner, H. P., & Ruppersburg, J. P. (1995) *Cell 80*, 149−154.

Ficker, E., Taglialatela, M., Wible, B. A., Henley, C. M., & Brown, A. M. (1994) *Science 266*, 1068−1027.

Heginbotham, L., Abramson, T., & MacKinnon, R. (1992) *Science 258*, 1152−1155.

Heginbotham, L., Lu, Z., Abramson, T., & MacKinnon, R. (1994) *Biophys. J. 66*, 1061−1067.

Hille, B. (1991) *Ionic Channels of Excitable Membranes*, Sinauer Associates, Inc., Sunderland, MA.

Ho, K., Nichols, C. G., Lederer, W. J., Lytton, J., Vassilev, P. M., Kanazirska, M. V., & Hebert, S. C. (1993) *Nature 362*, 31−38.

Horie, M., Isisawa, H., & Noma, A. (1987) *J. Physiol. 387*, 251−272.

Jencks, W. P. (1987) *Catalysis in Chemistry and Enzymology* (Jencks, W. P., Ed.) pp 243−281, Dover Publications, Inc., New York.

Kirsh, G. E., Pascual, J. M., & Shieh, C. (1995) *Biophys. J. 68*, 1804−1813

Kubo, Y., Baldwin, T. J., Yan, Y. N., & Jan, L. Y. (1993a) *Nature 362*, 127−132.

Kubo, Y., Reuveny, E., Slesinger, P. A., Jan, Y. N., & Jan, L. Y. (1993b) *Nature 364*, 802−806.

Li, M., Unwin, N., Stauffer, K., Jan, Y. N., & Jan, L. Y. (1994) *Cur. Biol. 4*, 110−115.

Liman, E. R., Tytgat, J., & Hess, P. (1992) *Neuron 9*, 861−871.

Lopatin, A. N., Makhina, E. N., & Nichols, C. G. (1994) *Nature 372*, 366−369.

Lu, Z., & MacKinnon, R. (1994) *Nature 371*, 243−246.

MacKinnon, R. (1991) *Nature (London) 350*, 232−235.

MacKinnon, R. (1995) *Neuron 14*, 889−892.

Matsuda, H., Saigusa, A., & Isisawa, H. (1987) *Nature 325*, 156−159.

Root, M. J., & MacKinnon, R. (1994) *Science 265*, 1852−1856.

Stanfield, P. R., Davies, N. W., Shelton, P. A., Sutcliffe, M. J., Khan, I. A., Brammar, W. J., & Conley, E. C. J. (1994) *J. Physiol. 478*, 1−6.

Vandenberg, C. A. (1987) *Proc. Natl. Acad. Sci. U.S.A. 84*, 2560−2564.

Wible, B. A., Taglialatela, M., Ficker, E., & Brown, M. (1994) *Nature 371*, 246−249.

BI9512152